Bulk Scattering Properties for the Remote Sensing of Ice Clouds.

1: Microphysical Data and Models

Bryan A. Baum[1], Andrew J. Heymsfield[2], Ping Yang[3], and

Sarah M. Thomas[4]

[1] NASA Langley Research Center, Hampton, VA

[2] National Center for Atmospheric Research, Boulder, CO

[3] Texas A&M University, College Station, TX

[4] Cooperative Institute for Meteorological Satellite Studies, Madison, WI

For submission to the

Journal of Applied Meteorology

Corresponding author: Dr. Bryan A. Baum, NASA LaRC, 1225 W. Dayton St., Madison, WI 53706. Phone: 608-263-3898; Fax: (608) 262-5974; E-mail: bryan.baum@ssec.wisc.edu

Abstract

This study reports on the use of aircraft and balloon-borne replicator *in situ* data obtained in midlatitude and tropical ice clouds as the basis for the development of bulk scattering models for use in satellite remote sensing applications. Part I entails the development of a comprehensive set of microphysical models based on in situ measurements of particle size distributions (PSDs). Two parameters are developed and examined: ice water content (*IWC*) and median mass diameter (D_m). Comparisons are provided between the *IWC* and D_m values derived from in situ measurements obtained during a series of field campaigns held in the midlatitude and tropical regions and those calculated from a set of modeled ice particles used for light scattering calculations. The ice particles considered in this study include droxtals, hexagonal plates, solid columns, hollow columns, aggregates, and 3-D bullet rosettes. We show that no single habit accurately replicates the derived *IWC* and D_m values, but a mixture of habits can significantly improve the comparison of these bulk microphysical properties. Additionally, we investigate the relationship between D_m and the effective particle size D_{eff}, defined as 1.5 times the ratio of ice particle volume to projected area for a given PSD. Based on these results, a subset of microphysical models is chosen as the basis for the development of ice cloud bulk scattering models in Part II of this study.

1. Introduction

We report on progress towards the development of a set of microphysical and optical models for use in the retrieval of global ice cloud properties by the MODerate resolution Imaging Spectroradiometer (MODIS) on the NASA Earth Observing System (EOS) Terra and Aqua platforms. Our goal is to form bulk scattering models for the purpose of retrieving ice cloud properties globally from satellite imagery, specifically cloud optical thickness and particle size. What is unique about this new formulation is the inclusion of more than one thousand *in situ* horizontally-averaged particle size distributions (PSDs) obtained from a variety of field campaigns in both midlatitude and tropical locales in addition to an extensive set of theoretical scattering properties for a variety of particle sizes and shapes.

In general, the microphysical models upon which most satellite ice cloud retrieval groups base their analyses make limited use of the *in situ* data that have been collected over the past several decades. For example, the cirrus scattering models used operationally since 1999 by the MODIS Atmospheres Team are based solely on midlatitude cirrus measurements (Baum et al. 2000; King et al. 2004). These Version 1 (hence V1) models are based on ice particle size distributions that have been discretized into five size bins, and use a mixture of habits consisting of four habits: hollow columns, plates, 2-D bullet rosettes, and aggregates. The habit distribution is the same for all models, and is a function only of particle size. The V1 cirrus models are used in conjunction with a radiative transfer model to develop static libraries of radiances/reflectances that are a function of optical thickness and particle size.

The development of a new set of midlatitude cirrus microphysical and scattering models was explored in Nasiri et al. (2002). The models used the same habits as for the V1 models but employed greater particle size discretization (27 size bins, compared to the original 5 size bins used in the operational MODIS cirrus models) and a characterization of the particle habit (shape) distributions. With the scattering property database developed for 27 size bins, the largest particle size bin was centered at 3500 μm.

A relevant question to ask is how well these midlatitude cirrus models represent the geographical and seasonal range of ice cloud properties found in nature. One major difference between midlatitude and tropical cirrus is that the tropical cirrus formed near centers of convection tend to contain more crystals of larger sizes than midlatitude, synoptically generated cirrus. For most synoptically-generated midlatitude cirrus, the largest crystal sizes measured are typically less than 1000 μm. Larger particles tend to settle out quickly due to the relatively low updraft velocities in the cloud layer. Updraft velocities in convection associated with the generation of tropical cirrus tend to be much higher, however, and the *in situ* measurements show that many large particles are typically present even in the uppermost regions of the cloud. This is also generally true for midlatitude ice clouds formed in areas of strong convection.

Recent research with tropical cirrus in-situ data has raised two issues. The first issue pertains to our discretization of a particle size distribution into a number of bins for the purposes of performing theoretical scattering calculations. Measurements of particle sizes in tropical cirrus, especially in the anvils of a cumulonimbus system near the convective cores, show the presence of particles up to cm in size. The presence of larger particles (i.e., > 3500 μm) in a particle size distribution should be properly accounted for in radia-

tive transfer calculations.

Another issue is the choice of a model representation of a habit appropriate for use in calculating the scattering properties of the extremely large crystals that form in areas of strong updrafts. The aggregate appears to be the most complex of the habits assumed in the scattering calculations, but as we will show later, this particular habit seems to be too dense to adequately represent tropical ice particles. For the scattering calculations, the aggregate is composed of a random number of columns attached to each other (Yang et al., 2000; Baum et al., 2000).

The basis for our research is the in situ data, specifically vertical distributions in particle size and habit, derived during various field missions (Heymsfield et al. 2002, 2003). The habits for which theoretical scattering calculations are used include hollow and solid columns, three-dimensional (3D) bullet rosettes, aggregates, plates, and droxtals. The droxtal has 20 facets and is designed to represent small quasi-spherical particles (Yang et al. 2003; Zhang et al. 2004). For each of the habits, a library has been developed of the scattering properties (including scattering phase function, single scatter albedo, extinction coefficient, extinction efficiency, asymmetry parameter, and size information) over an extended range of particle sizes (2 to 9,500 μm) and for a range of satellite wavelengths (0.4 μm to 12 μm). In addition to the bulk scattering properties, the models include ice water content (IWC) and two different particle sizes. The first is the effective particle size, which is based on the ensemble particle volume divided by the particle projected area for a given particle size and habit distribution. The second is the median mass diameter (D_m), defined as the size that divides the mass content of a particle size distribution in half. For a given value of D_m, half the mass is in particles of smaller size; half re-

sides in the larger particles.

Section 2 discusses the data and models used on the analyses. A comparison of scattering models at several wavelengths is provided in Section 3. Results from a comparison of in situ values to calculated *IWC* and median mass diameter (D_m) values is provided in Section 4, and section 5 summarizes the study. Based on the *in situ* particle size and habit distributions developed in Part I, a comprehensive set of scattering models are developed in Part II for the various types of ice clouds measured during the various field campaigns.

2. In-situ Microphysical Ice Cloud Data

a. Field Campaigns

A summary of the in situ data is presented in Table 1. Field campaigns located in the midlatitudes include the First ISCCP Regional Experiments (FIRE; ISCCP refers to the International Satellite Cloud Climatology Project) in Madison, WI in 1986 and Coffeyville, KS in 1991. Another midlatitude data set was derived in the vicinity of the Atmospheric Radiation Measurement (ARM) Southern Great Plains (SGP) site in Lamont, Oklahoma in March, 2000. The midlatitude cirrus generally had temperatures ranging from –65°C to –20°C, with visible optical thickness τ_{vis} values between 0.5 and 7. These ice cloud layers formed in association with synoptic-scale lifting.

In 1998 and 1999, four field campaigns were conducted under the auspices of the Tropical Rainfall Measuring Mission (TRMM). While the purpose of the campaigns was to evaluate the performance of the TRMM radar and radiometer retrieval algorithms, they also provided validation data for TRMM mesoscale and regional-scale models, as well as in-situ data from deep tropical cirrus and stratiform precipitating clouds. The tropical data

used in this study were obtained from the flights conducted in Kwajalein, Marshall Islands [Kwajalein Experiment: KWAJEX] in 1999. The tropical ice cloud temperatures ranged from –70°C to 0°C, with τ_{vis} values between 20 and 30, and formed in association with deep convection. Additionally, recent high-quality measurements have been acquired during the Cirrus Regional Study of Tropical Anvils and Cirrus Layers (CRYSTAL) Florida Area Cirrus Experiment (FACE) during a series of flights by the NASA WB57F aircraft and the University of North Dakota (UND) Citation. The CRYSTAL-FACE data used in this study were obtained from a flight track recorded off the coast of Nicaragua, and provides data from extremely cold cirrus (-76 °C to –58°C).

Imaging probes provide the aircraft-based size spectra measurements (Heymsfield et al. 2002). The Particle Measuring Systems, Inc. (PMS) 2D-C probes provide sizes from about 50 to 1000 μm. The 2D-C resolution is 25 μm for FIRE I but 33 μm for the other campaigns listed in Table 1. A PMS 2D-P probe measured larger particle sizes (1000 to more than 3000 μm) for the FIRE-I and ARM campaigns, with resolutions of 100 μm for FIRE-I and 200 μm for ARM. Additionally for the TRMM field campaign, large particle sizes from 1 to more than 30 mm were obtained from a Stratton Park Engineering Company (SPEC) high volume precipitation spectrometer (HVPS) probe with a resolution of 0.2 mm. A SPEC cloud particle imager (CPI) provided imagery for the ARM and TRMM campaigns over a range of sizes from 20 to 2000 μm with a 2-μm resolution. While the CPI probe provides spectacular imagery of the ice particles, its accuracy in measuring PSDs has yet to be established. Therefore the CPI data were not used to evaluate the numbers of small crystals in the PSDs.

Particle size distributions and habit imagery from FIRE II were obtained from bal-

loon-borne replicators. Particle sizes were obtained over a range from 10 to between 500 and 1000 μm, with a resolution of about 2 μm. The replicators measure size distributions and yield particle imagery reliably even for the smallest particles in the 10-20 μm diameter range. The continuous replicator observations are averaged over vertical distances of about 300 m (Heymsfield and Miloshevich 2003). Aircraft data from FIRE-II are also available, but the forward scattering spectrometer probe (FSSP) data, which provides particle sizes from 2 to 30 μm), are thought to be unreliable due to possible particle breakup in the probe inlet and are not used in this study. Further discussion of the measurement techniques and analysis of field campaign data are provided in Heymsfield and Miloshevich (2003) and Heymsfield et al. (2002).

b. Particle Size Distributions

Particle size distributions (PSD) are parameterized in the form of gamma distributions (Kosarev and Mazin, 1991; Mitchell, 1991; and Heymsfield et al., 2002) of the form:

$$n(D_{\max}) = N_0 D_{\max}^{\mu} e^{-\lambda D_{\max}}, \quad (1)$$

where D_{max} is the particle maximum dimension, $n(D)$ is the particle concentration per unit volume, N_0 is the intercept, λ is the slope, and μ is the dispersion. This relationship reduces to an exponential distribution when $\mu = 0$. The values for the intercept, slope, and dispersion were derived for each PSD by matching three moments; in this case, the first, second, and sixth moments were chosen as this set provided the best fit over the measured particle size range (Heymsfield et al. 2002).

The data are filtered by cloud temperature to ensure that the particle phase is ice, so that spectra are used from clouds that are colder than –25°C. Data from an ice detector

probe support the view that these particles are ice. The gamma fit parameters have been developed for more than 4000 PSDs measured in ice clouds in the midlatitudes, tropics and subtropics, but 1117 PSDs remain after filtering by cloud temperature, with a breakdown by field campaign shown in Table 2. Our focus is predominantly on data collected from Lagrangian spiral descents from the top to base of the ice cloud layers so that 1) optical depths can be estimated from the particle size distributions, 2) changes in particle size by height within the cloud column can be examined, a measurement more relevant to what a satellite observes, and 3) changes in particle shape in the vertical can be assessed. Each PSD from the aircraft observations represents a vertical depth within the cloud of about 30 m, while each replicator point represents roughly 300 m in the vertical. With Lagrangian descent spirals, the broadening of the PSDs may be attributed to the evolution of the size distributions through aggregation rather than size sorting.

Figure 1 shows a collection of PSDs based upon in situ data. The PSD from CRYSTAL-FACE, which involves a flight track off the coast of Nicaragua that sampled the coldest cloud in our data, displays the narrowest size distribution. Both the ARM and FIRE-II data were from fairly cold midlatitude cirrus, and have similar PSD shapes. The FIRE-I cirrus data typically come from warmer cirrus and display a broader range of particle sizes than for the colder clouds. The tropical cirrus shown in the TRMM PSD is typical of the tropical data, and exhibits more of an exponential size distribution behavior. The TRMM PSD is interesting for several reasons. Overall, there are more particles across the entire size range than for the midlatitude cirrus data. There are orders of magnitude more small particles for the TRMM PSD than for the other midlatitude cirrus PSDs. There also tend to be non-negligible numbers of large particles in the distribution,

although the maximum dimension range in this figure is abbreviated.

c. Inference of D_m and IWC from in-situ measurements

The two bulk cloud characteristics of interest in this study, D_m and *IWC*, are directly related to the PSDs (i.e., number concentration as a function of particle diameter) and the particle mass as a function of size. Recent studies examine the derivation of these bulk cloud properties from aircraft data (e.g., Heymsfield et al. 2002, 2004; Heymsfield and Miloshevich, 2003) and will be discussed only briefly here. The IWC was deduced from the *in situ* measurements from a mass dimension relationship and the size distributions. The mass dimension relationship was deduced from direct measurements of the IWC for clouds that were similar to those sampled during the various field programs (Heymsfield et al. 2004). The IWC calculations are thought to be accurate to better than 25%. The D_m was derived both analytically assuming the gamma size distribution fit parameters (Heymsfield et al. 2002) and from the distribution of particle mass with size as derived from the size distributions and the mass dimension relationship.

Heymsfield et al. (2002) provide the following simplified equations for D_m (cm) and *IWC* (g m^{-3}) that use the gamma PSD parameters of intercept, slope, and dispersion defined in Eq. (1) as well as the gamma function Γ:

$$D_m = \frac{2.90 + \mu}{\lambda}, \text{ and} \tag{2}$$

$$IWC = \frac{5700 N_0 \Gamma(3.2 + \mu)}{\lambda^{(3.2+\mu)}}. \tag{3}$$

d. Comparison to MODIS Version 1 PSDs

The set of 12 MODIS Version 1 (henceforth V1) PSDs is provided in Table 3. In

several of the V1 size distributions, there are roughly 1 to 2 orders of magnitude more particles of 20-μm size bin than of 50-μm size, and particle concentration drops off quickly as size increases. This strongly peaked PSD behavior is most similar to the CRYSTAL-FACE PSD, but even the CRYSTAL-FACE PSD does not have such a disparity in particle concentration over such a narrow size range. We note that earlier PSD spectra were derived in part from a combination of 2D-C/2D-P probe data in conjunction with the FSSP for small particles. There is now some question as to the reliability of the small particles counted by the FSSP, since large particles can break up upon entering the sampling volume, thereby elevating the number of small particles counted. The primary issue seems to be one of determining the appropriate number of very small particles to use in a PSD. The influence of the small particles on the single scatter albedo and asymmetry factor is shown in Part 2.

3. Simulated Ice Crystal Microphysical and Single Scattering Properties

Extensive libraries of microphysical and single scattering properties have been developed for a variety of ice crystal habits, including droxtals (Yang et al. 2003), two-and three-dimensional bullet rosettes, solid and hollow columns, plates, and aggregates (Yang et al., 2000). Calculations are performed for droxtals only up to 200 μm in maximum dimension. For all other habits, scattering properties are developed for particle sizes ranging from 2 to 9500 μm. The scattering calculations for all habits assume a random orientation. Microphysical properties for each habit include length, width, aspect ratio, volume and projected area as a function of maximum dimension.

As shown in Figure 1, the PSDs from tropical cirrus are much broader than for mid-latitude synoptic cirrus, meaning that more large particles are present in the distributions, and in higher concentrations. To accommodate the broader size distributions, the number of size bins has been increased from 27 (Nasiri et al. 2002) to 45, with the primary change being higher resolution for the largest particle sizes between 1000 and 9500 μm. For each of the habits, a library has been developed of the scattering properties (including scattering phase function, single scatter albedo, extinction coefficient, extinction efficiency, asymmetry parameter, and size information) for a range of satellite wavelengths between 0.4 μm and 13 μm. The scattering properties are discussed further in the companion paper.

For simulated ice particles, Figure 2 shows volume as a function of maximum dimension. For particles having D_{max} less than 200 μm (Fig. 2a), the droxtals have the highest volume, while the bullet rosettes tend to have the lowest volume. For habits with D_{max} between 200 and 2000 μm (Fig. 2b), aggregates tend to have the highest volume while the 3-D bullet rosettes have the lowest volume. For D_{max} greater than 2000 μm, aggregates have the highest volume while columns have the lowest volume.

4. Results

There are two issues that will have a significant effect on the bulk scattering/absorption properties of the ice cloud models: (1) the number of small particles, perhaps underrepresented because of *in situ* sampling issues, and (2) the number of large particles sometimes present near the cloud top in regions of strong convection, i.e., regions with relatively strong updrafts that tend to loft ice particles to high altitudes. The

large particles tend to have less influence on the single scattering properties in the visible and near-infrared bands than the more numerous small particles, but they are important for inferring the ice water content. Given the *in situ* D_m and *IWC* values for the size distributions deduced from the midlatitude and tropical field campaign data, it is a straightforward matter to compare these with the same parameters calculated from distributions of the simulated ice particles.

The total volume of ice per unit volume of air for a given distribution is given by

$$V_{Tot} = \sum_{h=1}^{M} \left[\int_{D\min}^{D\max} V(h,D)\, n(h,D)\, dD \right], \tag{4}$$

where D_{min} and D_{max} describe the minimum and maximum particle sizes in the distribution, $n(h,D)$ is the number distribution of a specific particle habit h for size D, and $V(h,D)$ is the volume of the habit h for size D, respectively. The total mass is obtained by multiplying the total volume by the bulk ice density (0.917 g cm^{-3}).

A first set of calculations is performed using the assumption of a single ice particle habit in the integration over each particle size distribution. As the ice volume per volume of air is a function of both habit and D_{max}, but especially ice particle concentration (which is proportional to the concentration intercept parameter N_o), one might expect that the relationship between *IWC* (which is proportional to N_o) and D_m (which is not proportional to N_o) could vary substantially given a range of particle size and habit distributions.

Results are presented assuming that the ice particle habit is entirely composed of aggregates (Fig. 3), 3-D bullet rosettes (Fig. 4), or solid columns (Fig. 5). In all three figures, the upper and lower panels show a comparison between values of IWC and D_m deduced from the *in situ* measurements (Section 2c, henceforth referred to as "in situ" in the

figures) and those derived from the simulated ice particles (Section 3, henceforth referred to as "calculated" in the figures). When the particles are all aggregates (Fig. 3), the IWC values from the midlatitude field campaigns (FIRE-I, FIRE-II, and ARM) tend to be distinct from the tropical data (CRYSTAL-FACE and TRMM). The calculated IWC values for CRYSTAL-FACE are lower than those deduced from the in situ data, while the opposite is true for the PSDs having the highest IWC values obtained from TRMM. However, the calculated values of D_m tend to be much higher than those estimated from the in situ data.

When 3-D bullet rosettes are employed (Fig. 4), the bifurcation in D_m between the midlatitude and tropical data is still apparent. The D_m values computed from TRMM using the 3-D bullet rosettes are uniformly higher than those inferred from the in-situ data. For all PSDs, however, the in situ *IWC* values are higher than those calculated using the 3-D bullet rosettes. Our interpretation of these results is that the 3-D bullet rosette formulation lacks the volume, and hence mass, that is observed in the *in-situ* data. Of our simulated ice particle habits, the 3-D bullet rosette is the only one that leads generally to an underestimate of *IWC* and an overestimate of D_m for the set of PSDs.

Figure 5 shows the same comparison, but with solid hexagonal columns used for the ice particles. The calculated *IWC* values tend to be higher by approximately 30% than those inferred from the measurements for most of the midlatitude cloud data, but the TRMM data tend to compare more closely. For D_m values less than 500 μm, the calculated values tend to agree closely with those inferred from the measurements. At higher D_m values, the in situ data have higher values than those calculated.

Based on these results, there may be some cause for optimism for developing a single

habit distribution that will increase the agreement between observed and calculated values for *IWC* and D_m. While microphysical and scattering properties are available for each habit, some consideration can be made as to making a more sensible choice in defining a habit distribution. For example, the droxtal seems to be a realistic choice to simulate the smallest crystals in a size distribution (< 60 μm). Observations have shown that neither plates nor columns tend to occur at sizes larger than 1000 μm. In general, the shapes of particles larger than perhaps 1000 μm tend to defy description, especially those noted in the tropical cases near centers of deep convection (i.e., anvil outflow).

While there may be many combinations of habits that optimize the comparison of measured to calculated values, we suggest one such distribution: D_{max} < 60 μm, 100% droxtals; 60 < D_{max} < 1000 μm, 15% 3-D bullet rosettes, 50% solid columns, 35% plates; 1000 < D_{max} < 2000 μm, 45% hollow columns, 45% solid columns, 10% aggregates; and D_{max} > 2000 μm, 97% 3-D bullet rosettes, 3% aggregates. Given this particular habit distribution, a comparison is provided in Figure 6 of calculated to measured *IWC* and D_m values. At higher *IWC* values, the measured values for TRMM tend to be lower than the calculated values, but are within a factor of 2. Overall, there seems to be general agreement in *IWC* and D_m over four orders of magnitude (10^{-4} to 10^{0} g m^{-3}).

One could argue that a habit distribution could be derived for each flight track that minimizes the difference between the *in situ* and calculated *IWC* and D_m values. Perhaps this could be investigated in future work. The primary purpose of this work is to provide a way to estimate particle size, and hence IWP, from remote sensing data that is more consistent with field measurements. We suggest that D_m may be a more useful parameter for numerical weather and climate modelers than some measure of effective particle size.

Nonetheless, if the retrievals are performed using a consistent set of models that are traceable to in situ measurements, it will be more straightforward to validate the data products.

For satellite retrievals, a common definition for the effective size of any particular PSD is provided by the effective diameter D_{eff}, which is proportional to the ratio of the total volume to the total projected area for a given particle size distribution. After Foot (1988) and Francis et al. (1994), D_{eff} is defined as

$$D_{eff} = \frac{3}{2} \frac{\sum_{h=1}^{M} \left[\int_{D_{\min}}^{D_{\max}} V(h,D)\, n(h,D)\, dD \right]}{\sum_{h=1}^{M} \left[\int_{D_{\min}}^{D_{\max}} A(h,D)\, n(h,D)\, dD \right]}, \tag{5}$$

where $A(h,D)$ is the projected area (per unit volume of air) of the crystal habit h for size D.

As both D_m (Eq. 2) and D_{eff} are independent of the particle number concentration, there should be some relationship between the two. Figure 7 provides a comparison between D_m and D_{eff}. As the larger particles contain most of the total mass, the value of D_m tends to be much larger than D_{eff}. The highest values of both D_{eff} and D_m occur for TRMM data, as one might expect given that the clouds are convective in origin. The range of D_{eff} is from 38 to 240 μm, while the range of D_m is from 48 to 2010 μm.

Summary

This study reports on the use of aircraft *in situ* data obtained from midlatitude and tropical ice clouds as the basis for the development of scattering models for use with satellite remote sensing applications. Part I entails the development of a comprehensive set

of microphysical models. Two parameters are developed: ice water content (*IWC*) and median mass diameter (D_m). Comparisons are provided between the *IWC* and D_m values obtained from in situ measurements obtained during a series of field campaigns held in the midlatitude and tropical regions and those calculated from a set of modeled ice crystals used for light scattering calculations. The modeled ice crystals include droxtals, hexagonal plates, solid columns, hollow columns, aggregates, and 3-D bullet rosettes. We show that no single habit model accurately replicates the *IWC* and D_m values inferred from the *in situ* measurements, but a habit mixture can significantly improve the comparison of derived to modeled microphysical properties. Based on these results, a subset of microphysical models is chosen as the basis for the development of ice cloud bulk scattering models in Part II of this study.

One observation regarding the use of the simulated habits is that the aggregate is a very dense particle, with the highest volume (and hence mass) at large crystal sizes. A habit distribution that relies primarily on aggregates will overestimate both D_m and *IWC*. The 3-D bullet rosette has the least volume/mass at intermediate particle sizes, and tends to underestimate the *IWC* for both midlatitude and tropical size distributions. A difference between the bullet rosette and the aggregate is that while *IWC* is underestimated, the D_m is overestimated with respect to the *in situ* data. Of the habits, the solid column compares most favorably with measurements of D_m and *IWC*. However, we show that a mixture of habits can improve the comparison of the *in situ* with calculated values.

Additionally, we investigate the relationship between D_m and the effective particle size D_{eff}, defined as 1.5 times the ratio of ice particle volume to projected area for a given PSD. While there is a monotonic relationship between the two parameters for the ARM,

FIRE-I, FIRE-II, and CRYSTAL-FACE data, the TRMM data seem to diverge slightly. The range of D_m values is much greater than for D_{eff} for the set of PSDs used in this study.

Acknowledgments

This research was sponsored by the Earth Science Enterprise. The authors specifically acknowledge the support and encouragement of Drs. Hal Maring and Donald Anderson of the NASA Radiation Sciences Program at NASA Headquarters. Dr. Yang's research is supported additionally by a National Science Foundation (NSF) CAREER Award research grant (ATM-0239605) provided by the NSF Physical Meteorology Program managed by Dr. William A. Cooper.

References

Baum, B. A., D. P. Kratz, P. Yang, S. Ou, Y. Hu, P. F. Soulen, and S. C. Tsay, 2000: Remote sensing of cloud properties using MODIS Airborne Simulator imagery during SUCCESS. I. Data and models. *J. Geophys. Res*., **105**, 11,767-11,780.

Field, P. R., and A. J. Heymsfield, 2003: Aggregation and scaling of ice crystal size distributions. J. Atmos. Sci., in press.

Heymsfield, A. J., A. Bansemer, P. R. Field, S. L. Durden, J. Stith, J. E. Dye, W. Hall, and T. Grainger, 2002: Observations and parameterizations of particle size distributions in deep tropical cirrus and stratiform precipitating clouds: Results from in situ observations in TRMM field campaigns. *J. Atmos. Sci*., **59**, 3457-3491.

Heymsfield, A. J., S. Matrosov, and B. A. Baum, 2003: Ice water path-optical depth relationships for cirrus and precipitating cloud layers. *J. Appl. Meteor*., **42**, 1369-1390.

Heymsfield, A. J., and L. M. Miloshevich, 2003: Parameterizations for the cross-sectional area and extinction of cirrus and stratiform ice cloud particles. *J. Atmos. Sci*., **60**, 936-956.

Heymsfield, A. J., A. Bansemer, C. Schmitt, C. Twohy, and M. R. Poellot, 2004: Effective ice particle densities derived from aircraft data. . *J. Atmos. Sci*., **61**, 982-1003.

King, M. D., S. Platnick, P. Yang, G. T. Arnold, M. A. Gray, J. C. Riédi, S. A. Ackerman, and K. N. Liou, 2004: Remote sensing of liquid water and ice cloud optical thickness and effective radius in the Arctic: Application of airborne multispectral MAS data. *J. Atmos. Oceanic Technol*., **21**, 857–875.

Kosarev, A. L., and I. P. Mazin, 1991: An empirical model of the physical structure of upper layer clouds. *Atmos. Res*., **26**, 213-228.

Mitchell, D. L., 1991: Evolution of snow-size spectra in cyclonic storms. Part II: Deviations from the exponential form. *J. Atmos. Sci*., **48**, 1885-1899.

Nasiri, S. L., B. A. Baum, A. J. Heymsfield, P. Yang, M. Poellot, D. P. Kratz, and Y. Hu, 2002: Development of midlatitude cirrus models for MODIS using FIRE-I, FIRE-II, and ARM *in-situ* data. *J. Appl. Meteor.,* **41**, 197-217.

Yang, P., K. N. Liou, K. Wyser, and D. Mitchell, 2000: parameterization of the scattering and absorption properties of individual ice crystals. *J. Geophys. Res*., **105**, 4699-4718.

Yang, P., B. A. Baum, A. J. Heymsfield, Y.X. Hu, H.-L. Huang, S. C. Tsay, and S. Ackerman, 2003: Single scattering properties of droxtals. *J. Quant. Spectrosc. Radiant. Transfer*, 79-80, 1159-1169.

Zhang, Z., P. Yang, G. W. Kattawar, S. C. Tsay, B. A. Baum, Y. X. Hu, A. J. Heymsfield, and J. Reichardt: Geometric optics solution for the scattering properties of droxtal ice crystals. *Appl. Opt*., **43**, 2490-2499.

List of Tables

Table 1: Data sources for in-situ measurements of ice cloud properties. Probe size ranges are: 2D-C, 40-1000 μm; 2D-P, 200-6400 μm; HVPS, 200–6100 μm; CPI, 20-2000 μm; Replicator, 10-800 μm.

Date	Location	Alt (m)	Temp (°C) (min,max)	Instruments	IWC (g m^{-3}) (min, max)	D_m (μm) (min,max)
19 Oct 1986	Madison, WI	8631-6992	-41 to -28	2D-C, 2D-P	2.60E-03, 2.87E-02	322, 554
22 Oct 1986	Madison, WI	8590-5435	-36 to -15	2D-C, 2D-P	3.15E-03, 9.42E-02	308, 995
25 Oct 1986	Madison, WI	8292-5601	-35 to –15	2D-C, 2D-P	2.06E-02, 1.04E-01	425, 1003
25 Oct 1986	Madison, WI	7652-5788	-30 to -16	2D-C, 2D-P	2.32E-03, 1.98E-01	287, 1151
28 Oct 1986	Madison, WI	7956-6262	-34 to -21	2D-C, 2D-P	6.05E-03, 1.02E-01	487, 1173
1 Nov 1986	Madison, WI	8964-6190	-43 to -21	2D-C, 2D-P	1.98E-03, 1.80E-02	198, 431
1 Nov 1986	Madison, WI	8800-5041	-41 to -18	2D-C, 2D-P	5.70E-03, 9.08E-02	231, 698
2 Nov 1986	Madison, WI	7786-4992	-36 to -19	2D-C, 2D-P	8.39E-03, 8.63E-02	259, 683
25 Nov 1991	Coffeyville, KS	9809-7313	-52 to -33	Replicator	2.30E-04, 4.98E-02	78, 223
26 Nov 1991	Coffeyville, KS	9816-6131	-54 to -24	Replicator	1.12E-04, 1.49E-02	82, 220
5 Dec 1991	Coffeyville, KS	12316-9381	-63 to -40	Replicator	2.90E-03, 1.41E-02	97, 254
5 Mar 2000	Lamont, OK	9969-8661	-52 to -40	2D-C, 2D-P, CPI	2.51E-03, 3.39E-02	139, 249
9 Mar 2000	Lamont, OK	9398-6699	-49 to -27	2D-C, 2D-P, CPI	1.59E-03, 1.63E-01	196, 1323
18 Aug 1999	Kwajalein, Marshall Islands	8423-5745	-25 to -6	2D-C, HVPS, CPI	3.20E-03, 6.13E00	333, 2450
22 Aug 1999	Kwajalein	11125-7340	-49 to -19	2D-C, HVPS, CPI	4.60E-02, 1.17E00	173, 2703
23 Aug 1999	Kwajalein	10403-6099	-42 to -9	2D-C, HVPS, CPI	4.86E-03, 5.47E00	136, 680
11 Sep 1999	Kwajalein	10057-4510	-39 to 0	2D-C, HVPS, CPI	3.80E-02, 1.08E00	150, 4255
26 July, 2002	Nicaragua	15161-13000	-76 to -58	VIPS	3.79E-04, 2.75E-03	50, 105

Table 2: Number of particle size distributions for each field campaign. Note that the total sample set has been filtered through the requirement that the cloud temperature be colder than –25°C.

Field Campaign	Location	Number of PSD's
FIRE-I	Madison, WI	246
FIRE-II	Coffeyville, KS	22
ARM	Lamont, OK	388
TRMM	Kwajalein, Marshall Islands	418
CRYSTAL-FACE	Nicaragua/Caribbean	39

Table 3: The twelve MODIS Version 1 particle size distributions. Note that there are five size bins, with particle densities in units of # particles m^{-3} μm^{-1}.

Model	**20 μm**	**50 μm**	**120 μm**	**300 μm**	**750 μm**
Cold Ci	8.600e+3	7.516e+1	8.367e-1	5.867e-2	3.994e-3
Ci at T =-60°C	3.034e+3	8.638e+1	2.877e+0	8.175e-2	2.323e-3
Cs	6.700e+3	9.758e+2	3.243e+1	1.497e+0	0.000e+0
Warm Ci	2.005e+4	7.028e+2	3.694e+1	4.807e+0	1.414e-1
Ci at T =-20°C	1.032e+4	6.691e+2	4.899e+1	3.175e+0	2.058e-1
Ci at T=-40°C	7.398e+3	6.125e+2	5.667e+1	4.692e+0	2.005e-1
1 Nov 1986	8.076e+2	1.894e+2	4.183e+1	4.813e+0	4.092e-2
2 Nov 1986	7.892e+2	2.141e+2	4.749e+1	1.750e+1	1.921e-1
22 Oct 1986	1.434e+3	3.026e+2	3.663e+1	1.131e+1	5.857e-1
25 Oct 1986	1.847e+3	4.256e+2	5.594e+1	1.862e+1	1.191e+0
Ci Uncinus	5.710e+3	1.280e+3	1.294e+2	4.110e+1	5.976e+0
28 Oct 1986	9.566e+2	2.441e+2	3.769e+1	1.051e+1	5.789e-1

List of Figures

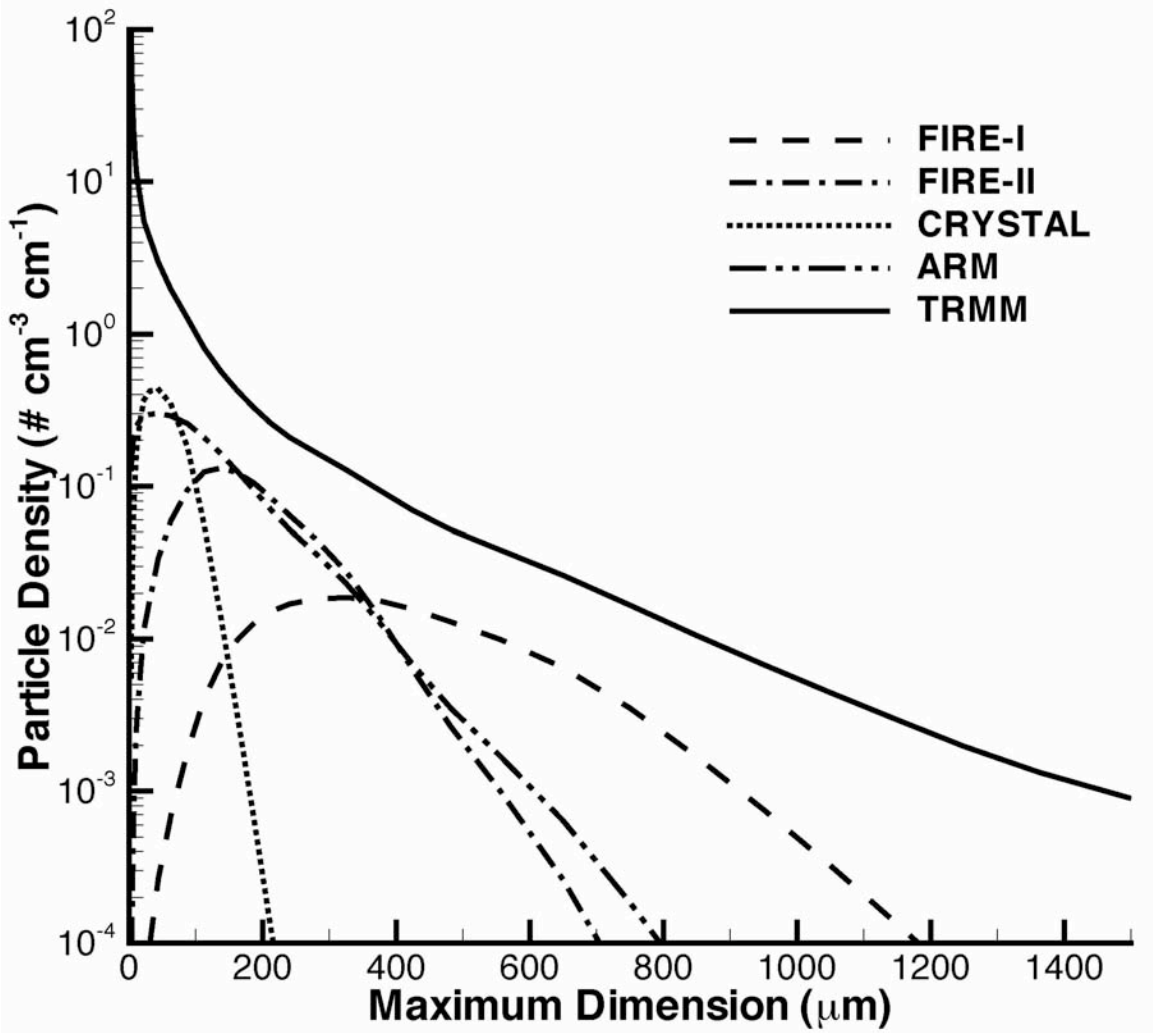

Figure 1. Sample of particle size distributions selected from the various field experiments. While the FIRE-I, FIRE-II, ARM, and CRYSTAL data tend to have the appearance of the more general "gamma" distribution, the TRMM PSD follows an exponential particle distribution.

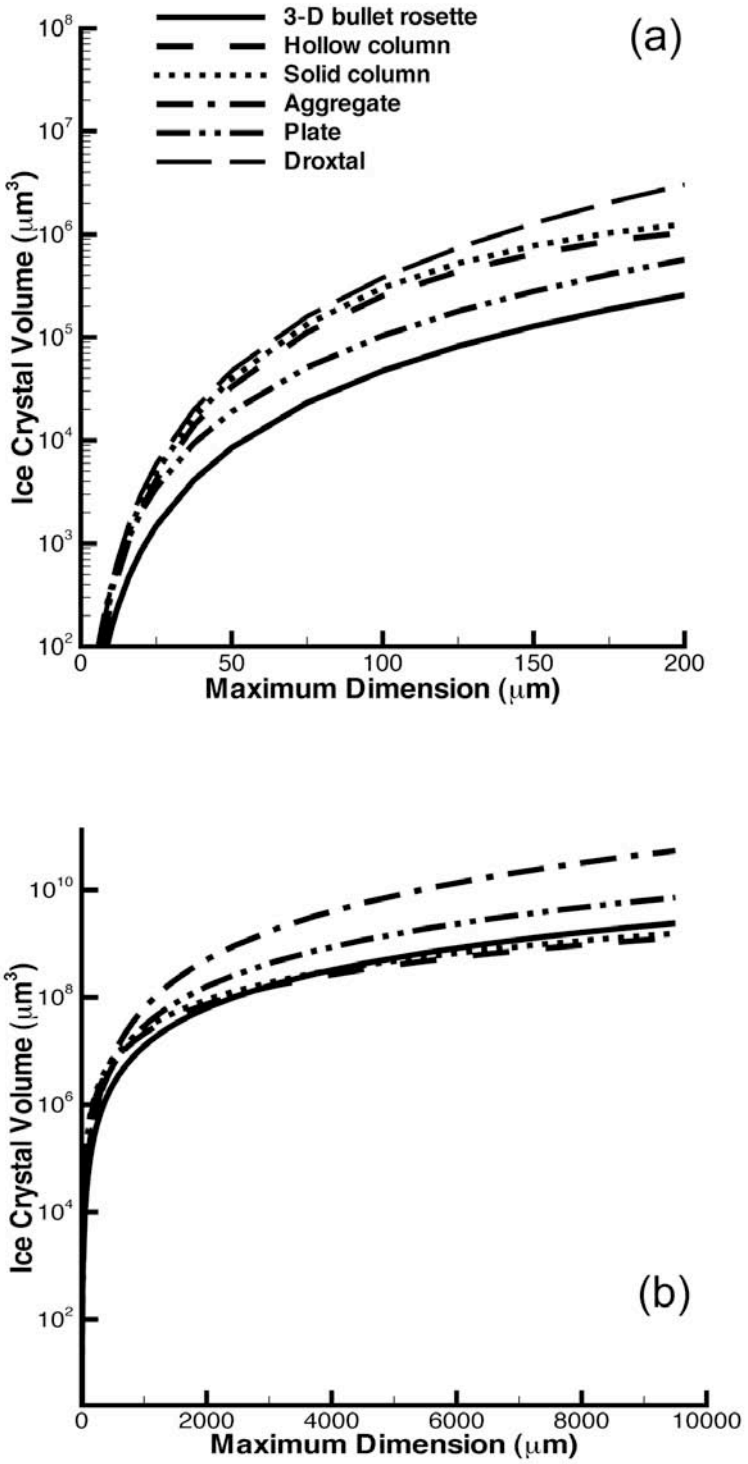

Figure 2. Ice crystal volume as a function of habit and crystal maximum dimension D_{max}. Droxtal properties have been calculated for small particles only (D_m < 200 μm).

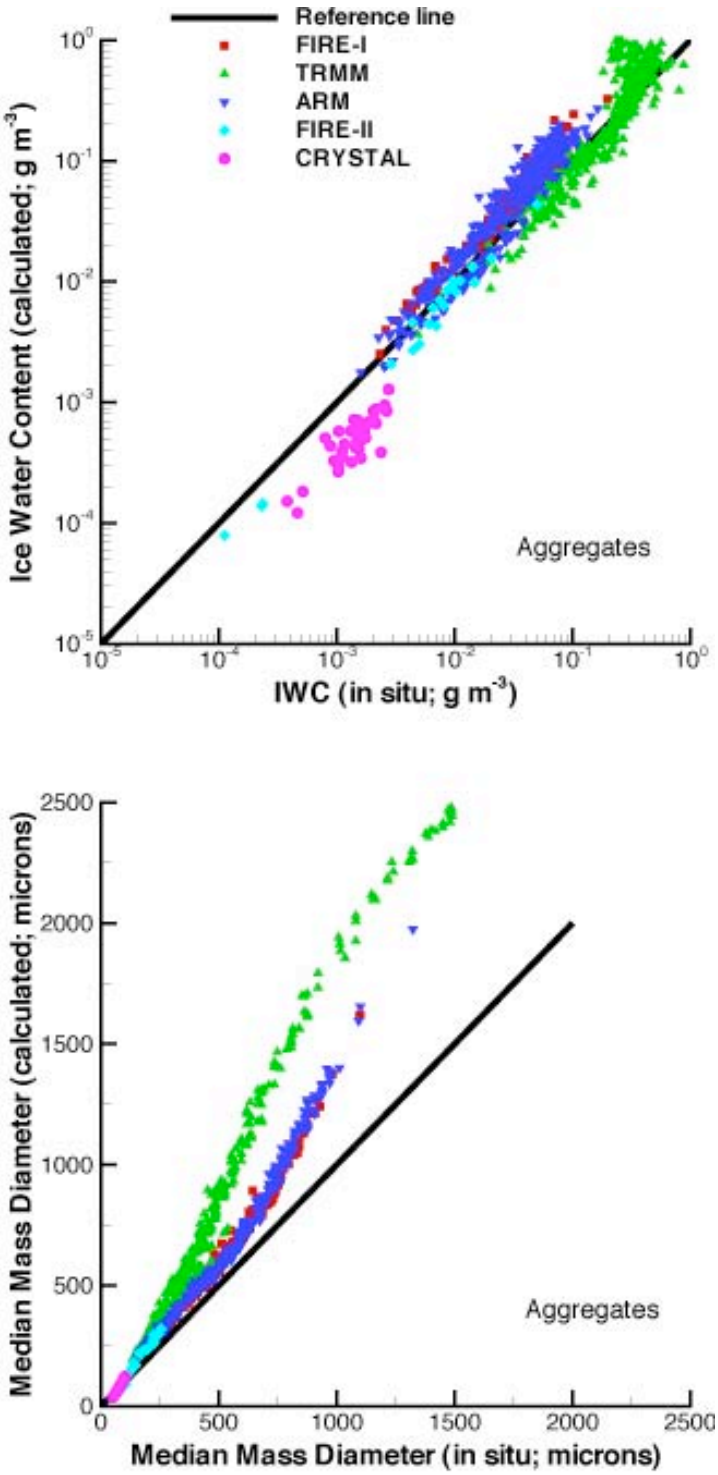

Figure 3. Comparison of in-situ to calculated ice water content (IWC) and median mass diameter (D_m) for each of the size distributions obtained from the FIRE-I, FIRE-II, ARM, TRMM, and CRYSTAL field campaigns. The habit distribution is as follows: D_{max} < 60 μm, 100% droxtals; D_{max} > 60 μm, 100% aggregates.

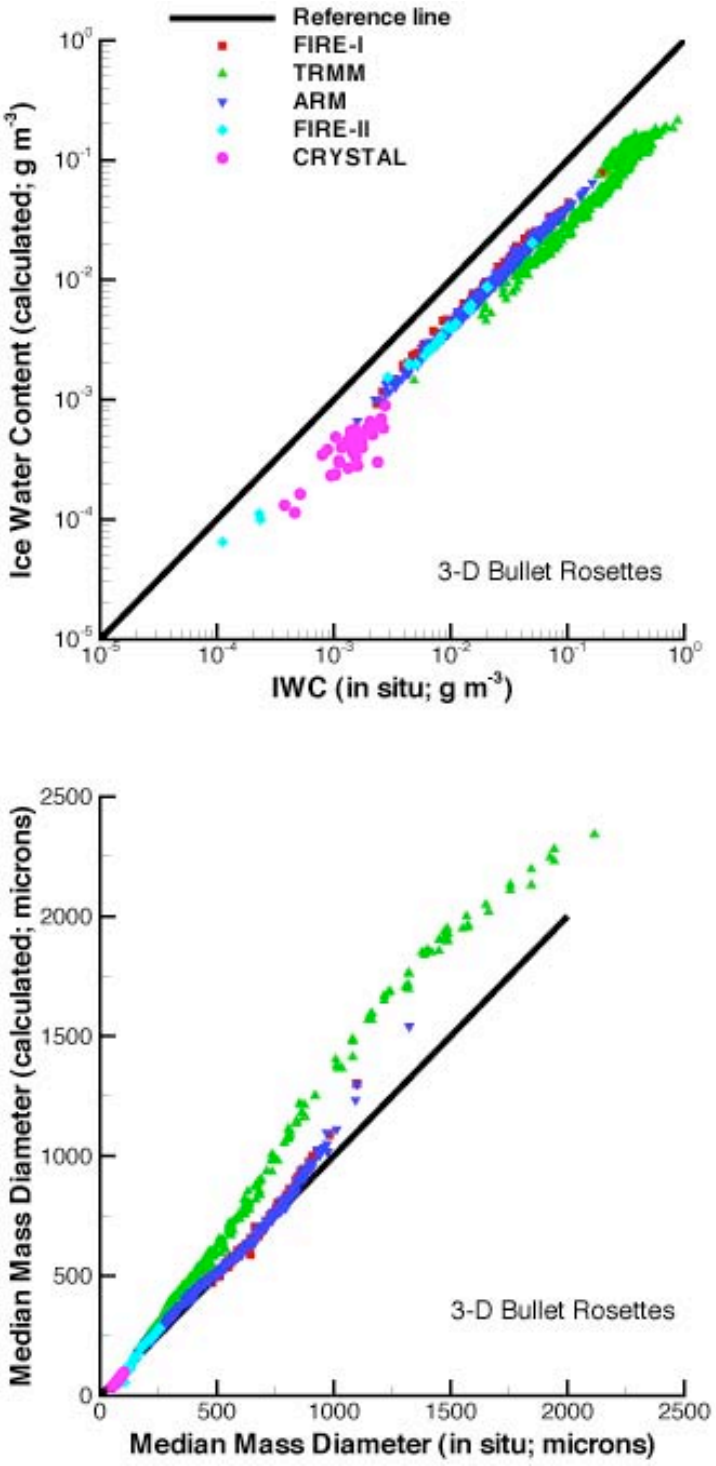

Figure 4. Comparison of in-situ to calculated ice water content (IWC) and median mass diameter (D_m) for each of the size distributions obtained from the FIRE-I, FIRE-II, ARM, TRMM, and CRYSTAL field campaigns. The habit distribution is as follows: $D_{max} < 60$ μm, 100% droxtals; $D_{max} > 60$ μm, 100% 3-D bullet rosettes.

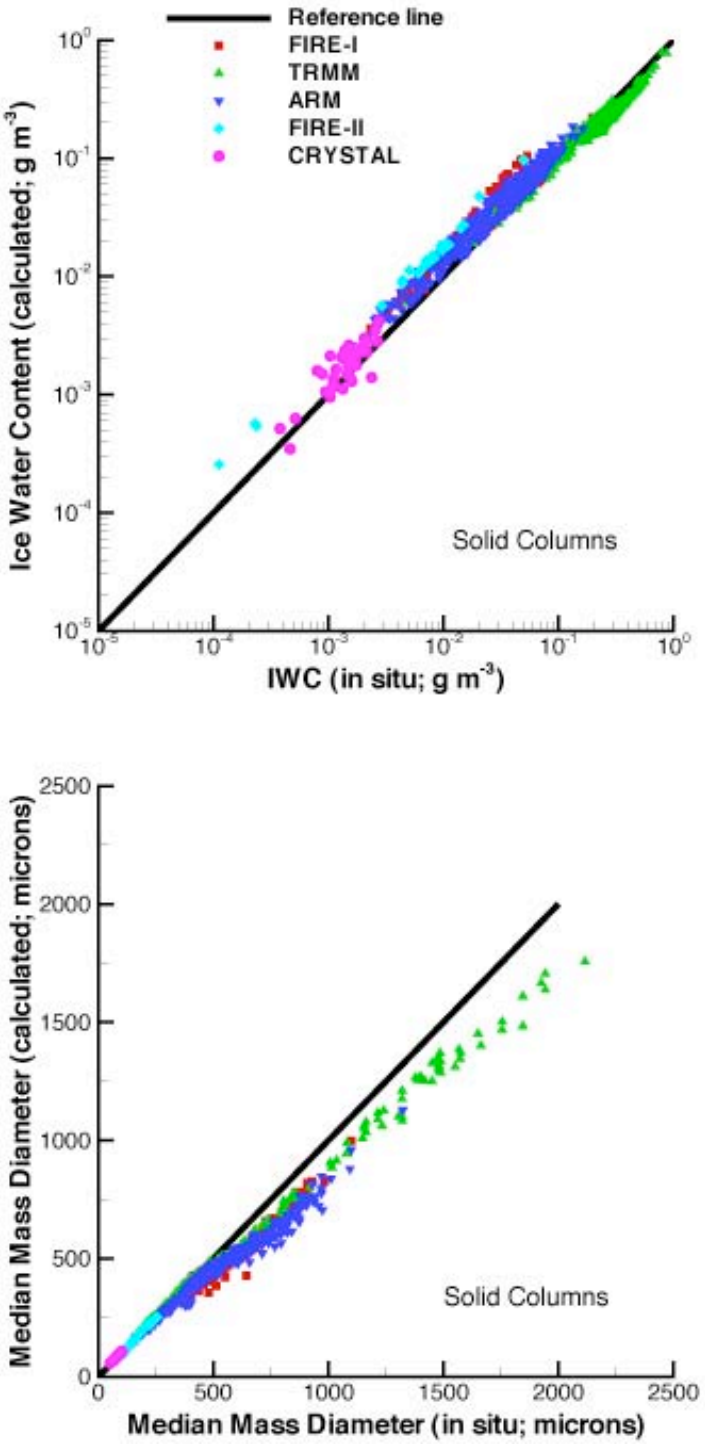

Figure 5. Comparison of in-situ to calculated ice water content (IWC) and median mass diameter (D_m) for each of the size distributions obtained from the FIRE-I, FIRE-II, ARM, TRMM, and CRYSTAL field campaigns. The habit distribution is as follows: D_{max} < 60 μm, 100% droxtals; D_{max} > 60 μm, 100% solid columns.

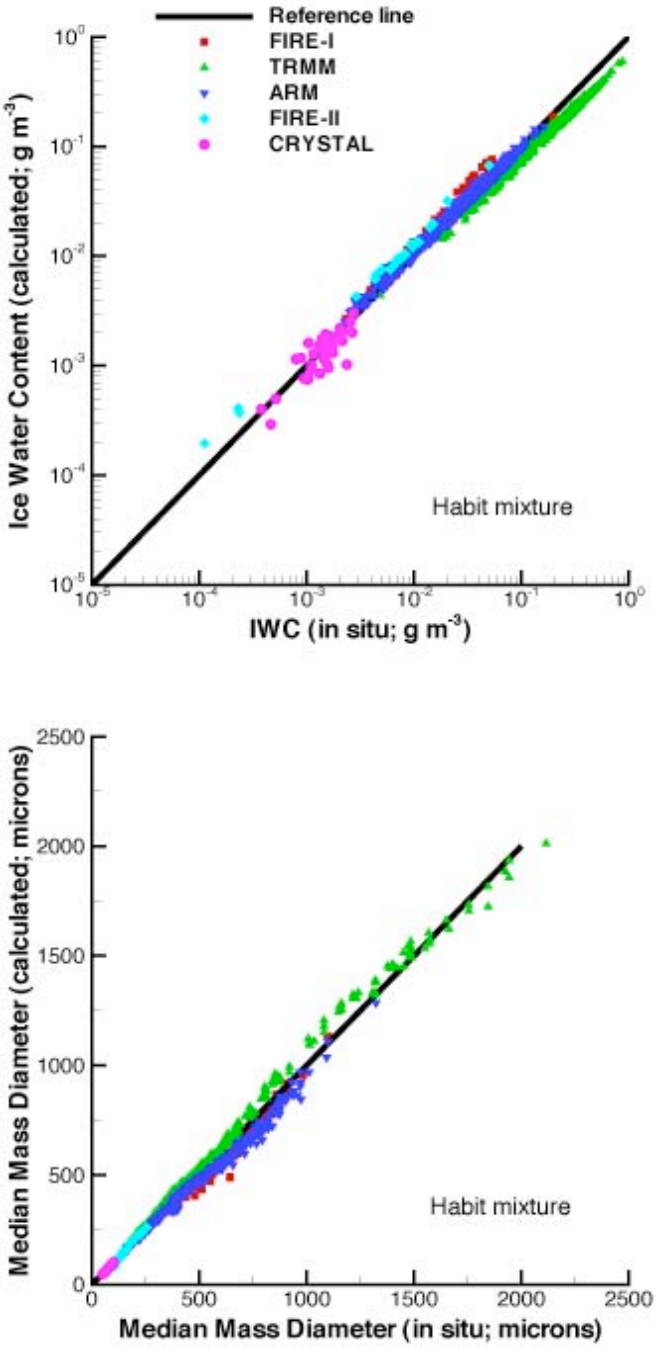

Figure 6. Comparison of in-situ to calculated ice water content (IWC) and median mass diameter (D_m) for each of the size distributions obtained from the FIRE-I, FIRE-II, ARM, TRMM, and CRYSTAL field campaigns. The habit distribution is as follows: $D_{max} < 60$ μm, 100% droxtals; $60 < D_{max} < 1000$ μm, 15% 3-D bullet rosettes, 50% solid columns, 35% plates; $1000 < D_{max} < 2000$ μm, 45% hollow columns, 45% solid columns, 10% aggregates; and $D_{max} > 2000$ μm, 97% 3-D bullet rosettes, 3% aggregates.

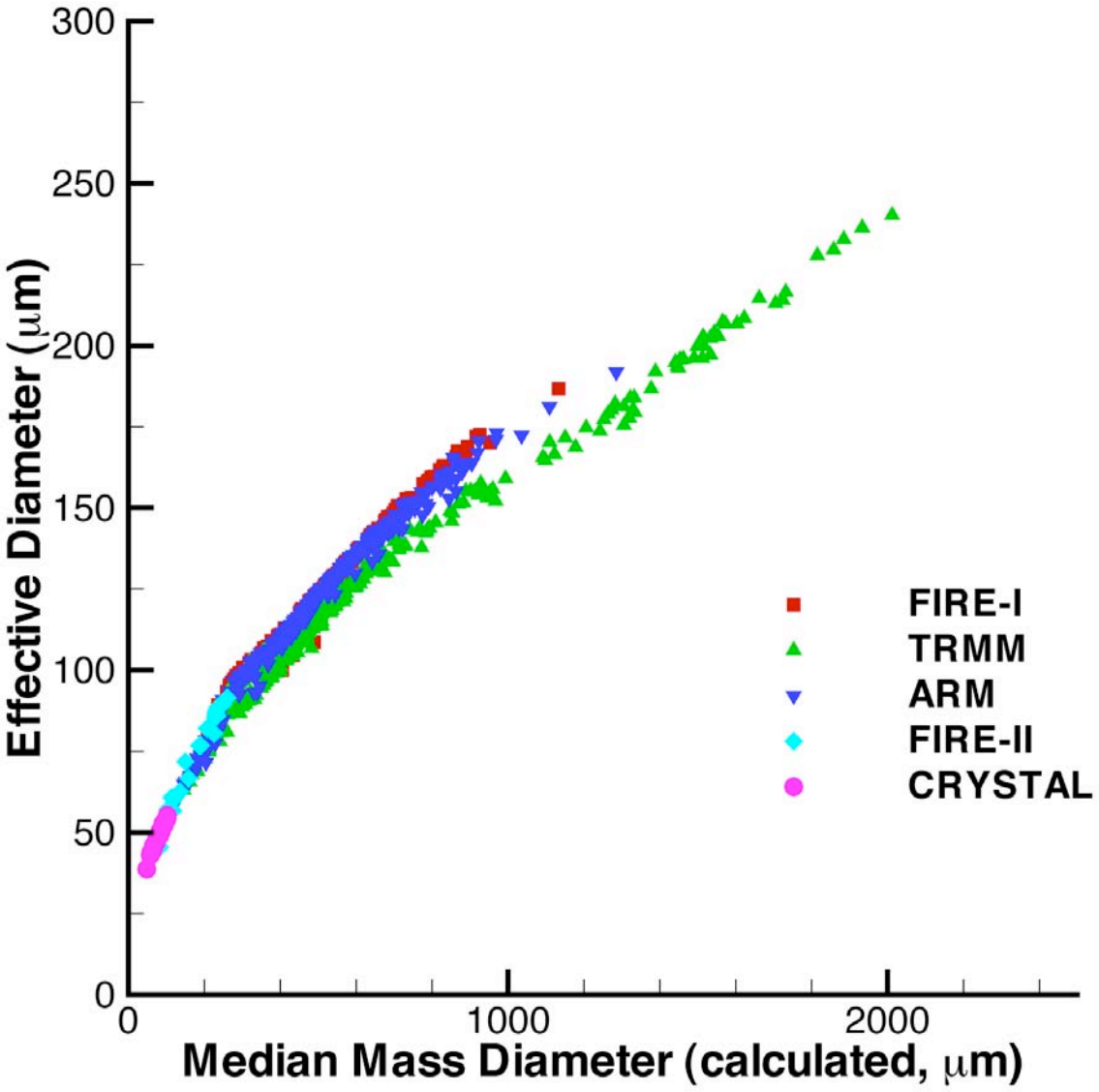

Figure 7. Comparison of effective diameter D_e to median mass diameter D_m.